Electronic Supplementary Information

Protein Corona Alleviates Adverse Biological Effects of Nanoplastics in Breast Cancer Cells

Siyao Xiao [a], Junbiao Wang [b], Luca Digiacomo [a], Augusto Amici [b], Valentina De Lorenzi[c], Licia Anna Pugliese[c], Francesco Cardarelli [c], Andrea Cerrato,[d] Aldo Laganà,[d] Lishan Cui,[e,f] Massimiliano Papi,[e,f] Giulio Caracciolo [a], Cristina Marchini *[b], Daniela Pozzi *[a]

[a] NanoDelivery Lab, Department of Molecular Medicine, Sapienza University of Rome, Viale Regina Elena 291, 00161 Rome, Italy
[b] School of Biosciences and Veterinary Medicine, University of Camerino, 62032 Camerino, Italy
[c] Laboratorio NEST, Scuola Normale Superiore, Piazza San Silvestro 12, 56127 Pisa, Italy
[d] Department of Chemistry, Sapienza University of Rome, P.le A. Moro 5, 00185 Rome, Italy
[e] Department of Neuroscience, Catholic University of the Sacred Heart, Largo Francesco Vito 1, Rome 00168, Italy
[f] Fondazione Policlinico Universitario A. Gemelli IRCSS, Rome 00168, Italy

*** corresponding authors:** cristina.marchini@unicam.it (C.M.); daniela.pozzi@uniroma1.it (D.P.)

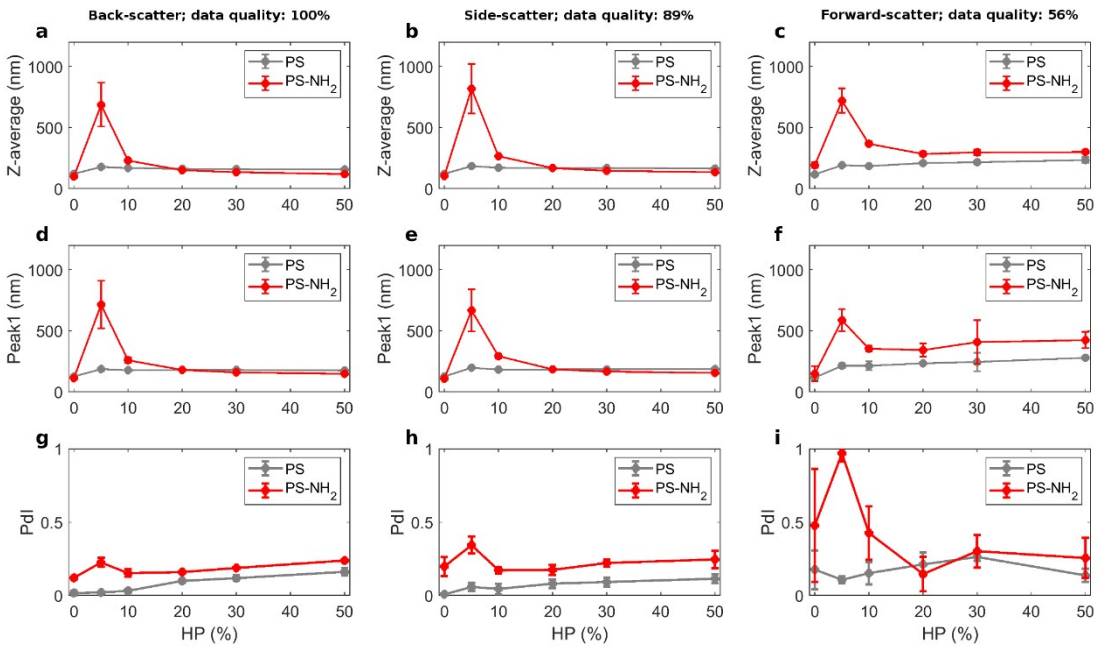

Figure S1. DLS data of NPs upon exposure to HP, at three different scattering angles, i.e. 173° (back scattering), 90° (side scattering), and 17° (forward scattering). Data quality is evaluated as percentage of replicates with good quality reports, as indicated by the Malvern Software for DLS data acquisition. (a, b, c) Z-average, (d-f) peak location, and (g-i) PdI as functions of HP percentage.

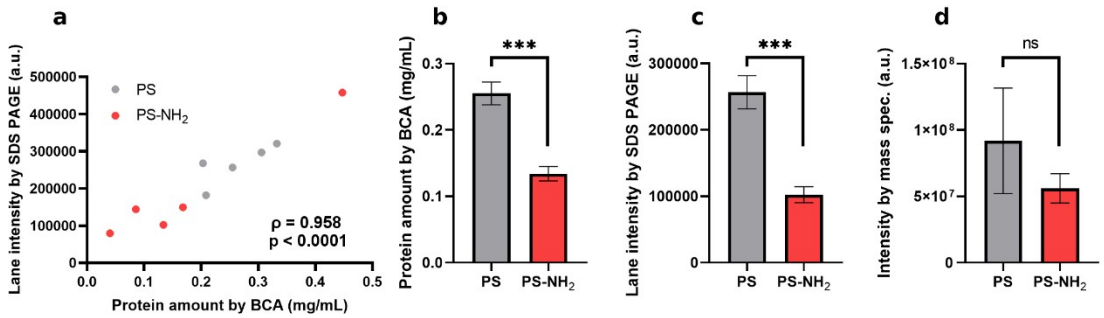

Figure S2. (a) Correlation analysis between total protein amount in the hard corona of NPs by BCA assay and total lane intensity by SDS-PAGE. (b) protein amount by BCA, (c) total lane intensity by SDS-PAGE, and (d) intensity by nano-liquid chromatography mass spectrometry experiments for unmodified PS NPs and NH2-PS NPs upon exposure to 30% HP. The obtained results clearly indicate a robust correspondence between BCA, SDS-PAGE, and proteomics analyses.

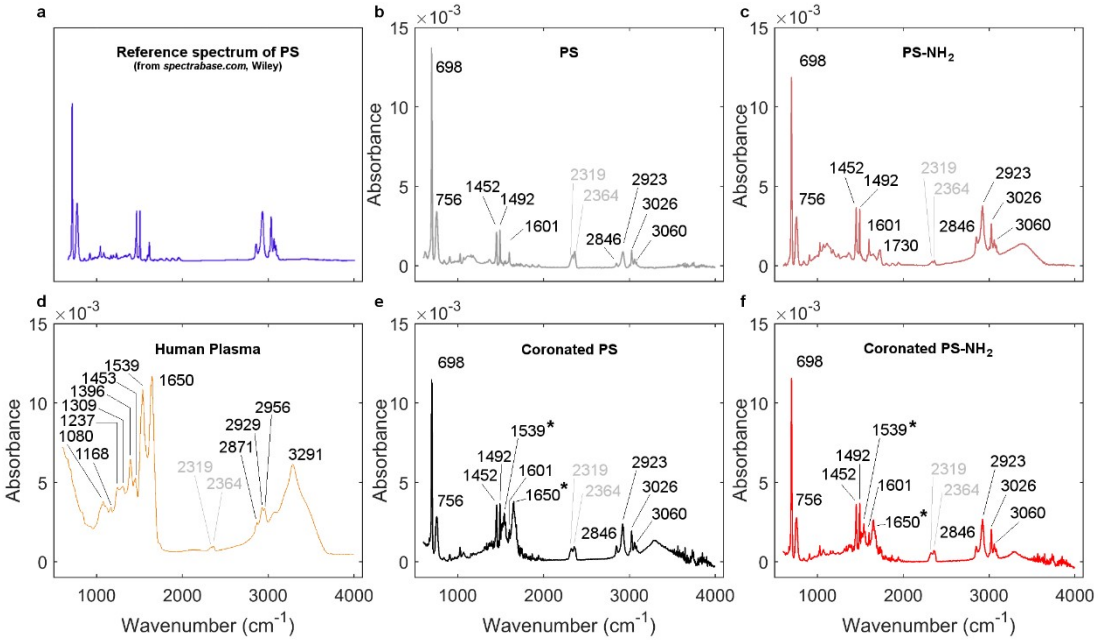

Figure S3. FT-IR analysis of pristine and coronated NPs. (a) Reference FT-IR spectrum for Polystyrene, as reported on spectrabase.com (John Wiley & Sons, Inc.). FT-IR spectra of (b) PS, (c) PS-NH_2, (d) HP, (e) coronated PS, and (f) coronated PS-NH_2. Asterisks indicate HP peaks found in coronated samples and absent in pristine systems.

FT-IR spectroscopy provided a chemical characterization of both pristine systems and nanoparticles (NPs) exposed to 30% human plasma (HP), hereafter referred to as coronated particles. Results are shown in Fig. S3 and clearly indicate that coronated particles exhibit distinct HP signatures in their FT-IR spectra, demonstrating the formation of a protein corona on their surfaces. In detail, a nominal spectrum for Polystyrene (Fig. S3 a) was used as a reference. Our experimental data for PS (Fig. S3 b) and PS-NH_2 showed very good agreement with the reference. The main discriminant feature between them was a characteristic peak for the amine-modified system, located at 1730 cm^{-1}, likely attributable to surface functionalization. Other notable peaks included C-H out-of-plane bending vibration absorption (698 cm^{-1}, 756 cm^{-1}), C=C stretching vibration absorption (1450 cm^{-1}, 1490 cm^{-1}, 1600 cm^{-1}), and C-H stretching vibration absorption (from 2800 cm^{-1} to 3060 cm^{-1}) [1]. Besides the observed matching between the experimental spectra and the reference, we note that the measured FT-IR curve for PS is very similar to those reported in previous studies. For instance, the measured locations of FT-IR peaks in Fig. S3 strongly agree with those reported by Fang et al. in 2009 [1]. Similarly, the experimental FT-IR spectrum for HP (Fig. S3 d) matches those reported in previous studies, e.g. by Araùjo et al in 2002[2]. HP spectrum exhibited a large number of absorption peaks, due to the intrinsic complexity of the biological specimen. Among them, two main contributions can be distinugished, i.e. amide I (1650 cm^{-1}, C=O stretching vibration) and amide II band

(1539 cm^{-1}, N–H bending and C–N stretching) [3]. Notably, these two peaks are differentially present in the spectra of both coronated PS (Fig. S3 e) and coronated PS-NH_2 (Fig. S3 f) systems, and provide deemonstration of corona formation at the particle surface.

Table S1 List of identified proteins in the corona of unmodified PS NPs and NH-2 PS NPs by nano-liquid chromatography tandem mass spectrometry analysis. Proteins are sorted in decreasing order of RPAs for the amine-modified systems.

Protein name	Abbreviation	RPA (%) in PS NP corona	RPA (%) in PS-NH2 corona
Apolipoprotein A-I	APOA1	19.20% ± 4.74%	21.11% ± 0.30%
Apolipoprotein A-II	APOA2	16.98% ± 4.01%	13.25% ± 1.17%
Apolipoprotein C-III	APOC3	3.80% ± 3.36%	13.13% ± 0.28%
Serum albumin	ALB	3.76% ± 0.71%	11.39% ± 0.42%
Apolipoprotein C-II	APOC2	2.74% ± 2.56%	7.31% ± 0.70%
Vitronectin	VTN	0.27% ± 0.22%	6.67% ± 1.01%
Clusterin	CLU	0.43% ± 0.27%	3.91% ± 0.06%
Apolipoprotein C-I	APOC1	1.53% ± 0.67%	2.85% ± 0.10%
Apolipoprotein E	APOE	1.28% ± 0.47%	2.50% ± 0.40%
Ig kappa chain C region	IGKC	1.22% ± 0.80%	2.15% ± 0.11%
Apolipoprotein A-IV	APOA4	0.08% ± 0.00%	1.71% ± 0.39%
Ig gamma-1 chain C region	IGHG1	0.80% ± 0.99%	1.29% ± 0.40%
Keratin, type II cytoskeletal 1	KRT1	0.51% ± 0.03%	1.08% ± 0.12%
Prothrombin	F2	0.00% ± 0.00%	1.07% ± 0.02%
Serum paraoxonase/arylesterase 1	PON1	0.00% ± 0.00%	0.96% ± 0.04%
Fibrinogen gamma chain	FGG	13.05% ± 0.51%	0.94% ± 0.14%
C4b-binding protein alpha chain	C4BPA	0.34% ± 0.00%	0.89% ± 0.04%
Ig gamma-3 chain C region	IGHG3	1.66% ± 0.05%	0.82% ± 0.03%
Ig mu chain C region	IGHM	0.17% ± 0.10%	0.71% ± 0.15%
Fibrinogen alpha chain	FGA	11.51% ± 1.68%	0.68% ± 0.15%
Immunoglobulin lambda-like polypeptide 5	IGLL5	3.91% ± 0.92%	0.67% ± 0.12%
Keratin, type I cytoskeletal 10	KRT10	0.37% ± 0.04%	0.60% ± 0.13%
Immunoglobulin lambda constant 3	IGLC3	2.79% ± 0.58%	0.59% ± 0.11%
Fibrinogen beta chain	FGB	6.38% ± 4.22%	0.54% ± 0.06%
Complement C4-B	C4B;C4A	0.13% ± 0.05%	0.48% ± 0.06%
Keratin, type I cytoskeletal 9	KRT9	0.14% ± 0.01%	0.34% ± 0.07%
Haptoglobin	HP	0.48% ± 0.26%	0.33% ± 0.19%
Hyaluronan-binding	HABP2	0.00% ± 0.00%	0.31% ± 0.07%

protein 2								
Ig alpha-1 chain C region	IGHA1;IGHA2	0.22%	±	0.11%	0.30%	±	0.00%	
Alpha-1-antitrypsin	SERPINA1	0.10%	±	0.05%	0.20%	±	0.06%	
Serum amyloid A-4 protein	SAA4	0.31%	±	0.06%	0.18%	±	0.03%	
Complement C1q subcomponent subunit C	C1QC	0.80%	±	0.12%	0.15%	±	0.01%	
Complement C3	C3	0.59%	±	0.06%	0.13%	±	0.02%	
Ig gamma-2 chain C region	IGHG2	0.07%	±	0.08%	0.11%	±	0.03%	
Keratin, type II cytoskeletal 2 epidermal	KRT2	0.15%	±	0.03%	0.11%	±	0.05%	
Apolipoprotein D	APOD	0.00%	±	0.00%	0.09%	±	0.08%	
Apolipoprotein C-IV	APOC4	0.01%	±	0.01%	0.09%	±	0.12%	
Serotransferrin	TF	0.29%	±	0.18%	0.08%	±	0.00%	
Ceruloplasmin	CP	0.01%	±	0.02%	0.06%	±	0.01%	
Serum amyloid A-1 protein	SAA1;SAA2	0.16%	±	0.20%	0.04%	±	0.06%	
Properdin	CFP	0.20%	±	0.03%	0.03%	±	0.04%	
Vitamin K-dependent protein S	PROS1	0.02%	±	0.02%	0.03%	±	0.01%	
Alpha-2-HS-glycoprotein	AHSG	0.15%	±	0.06%	0.02%	±	0.00%	
Complement C1s subcomponent	C1S	0.03%	±	0.01%	0.01%	±	0.00%	
Glutathione peroxidase 3	GPX3	0.02%	±	0.02%	0.01%	±	0.02%	
Protein AMBP	AMBP	0.00%	±	0.00%	0.01%	±	0.02%	
Apolipoprotein B-100	APOB	0.01%	±	0.01%	0.01%	±	0.00%	
Alpha-2-macroglobulin	A2M	0.04%	±	0.01%	0.01%	±	0.00%	
Inter-alpha-trypsin inhibitor heavy chain H2	ITIH2	0.03%	±	0.01%	0.01%	±	0.01%	
Apolipoprotein L1	APOL1	0.01%	±	0.02%	0.01%	±	0.01%	
Apolipoprotein(a)	LPA	0.00%	±	0.00%	0.01%	±	0.01%	
Complement factor H	CFH	0.23%	±	0.06%	0.01%	±	0.00%	
Complement C1r subcomponent	C1R	0.05%	±	0.00%	0.00%	±	0.01%	
Keratin, type I cytoskeletal 13	KRT13	0.00%	±	0.00%	0.00%	±	0.00%	
Inter-alpha-trypsin inhibitor heavy chain H1	ITIH1	0.01%	±	0.02%	0.00%	±	0.00%	
Tetranectin	CLEC3B	0.03%	±	0.04%	0.00%	±	0.00%	
Hornerin	HRNR	0.00%	±	0.00%	0.00%	±	0.00%	
Complement component C9	C9	0.00%	±	0.00%	0.00%	±	0.00%	
Gelsolin	GSN	0.31%	±	0.00%	0.00%	±	0.00%	

Ig lambda chain V region 4A	IGLV7-46	0.05%	±	0.07%	0.00%	±	0.00%
Ig lambda chain V-III region LOI	IGLV3-9;IGLV3-12	0.01%	±	0.01%	0.00%	±	0.00%
Ig lambda-7 chain C region	IGLC7	0.03%	±	0.04%	0.00%	±	0.00%
CD5 antigen-like	CD5L	0.01%	±	0.00%	0.00%	±	0.00%
Plasminogen	PLG	0.06%	±	0.02%	0.00%	±	0.00%
Complement factor B	CFB	0.03%	±	0.02%	0.00%	±	0.00%
Alpha-1-antichymotrypsin	SERPINA3	0.01%	±	0.01%	0.00%	±	0.00%
Complement C5	C5	0.00%	±	0.00%	0.00%	±	0.00%
Kininogen-1	KNG1	0.06%	±	0.05%	0.00%	±	0.00%
Ig kappa chain V-III region B6	IGKV3D-20	0.03%	±	0.01%	0.00%	±	0.00%
Ig lambda chain V-III region SH		0.04%	±	0.06%	0.00%	±	0.00%
Ig gamma-4 chain C region	IGHG4	0.05%	±	0.00%	0.00%	±	0.00%
Complement C1q subcomponent subunit A	C1QA	0.39%	±	0.13%	0.00%	±	0.00%
Complement C1q subcomponent subunit B	C1QB	0.43%	±	0.31%	0.00%	±	0.00%
Beta-2-glycoprotein 1	APOH	0.47%	±	0.01%	0.00%	±	0.00%
Fibronectin	FN1	0.08%	±	0.03%	0.00%	±	0.00%
Hemopexin	HPX	0.03%	±	0.01%	0.00%	±	0.00%
Plasma kallikrein	KLKB1	0.04%	±	0.04%	0.00%	±	0.00%
Histidine-rich glycoprotein	HRG	0.01%	±	0.02%	0.00%	±	0.00%
Heparin cofactor 2	SERPIND1	0.01%	±	0.00%	0.00%	±	0.00%
Alpha-2-antiplasmin	SERPINF2	0.01%	±	0.00%	0.00%	±	0.00%
Hemoglobin subunit alpha	HBA1;HBZ	0.07%	±	0.04%	0.00%	±	0.00%
Complement factor H-related protein 1	CFHR1	0.04%	±	0.00%	0.00%	±	0.00%
Inter-alpha-trypsin inhibitor heavy chain H4	ITIH4	0.63%	±	0.30%	0.00%	±	0.00%
Testis- and ovary-specific PAZ domain-containing protein 1	TOPAZ1	0.01%	±	0.01%	0.00%	±	0.00%
Proteoglycan 4	PRG4	0.01%	±	0.01%	0.00%	±	0.00%

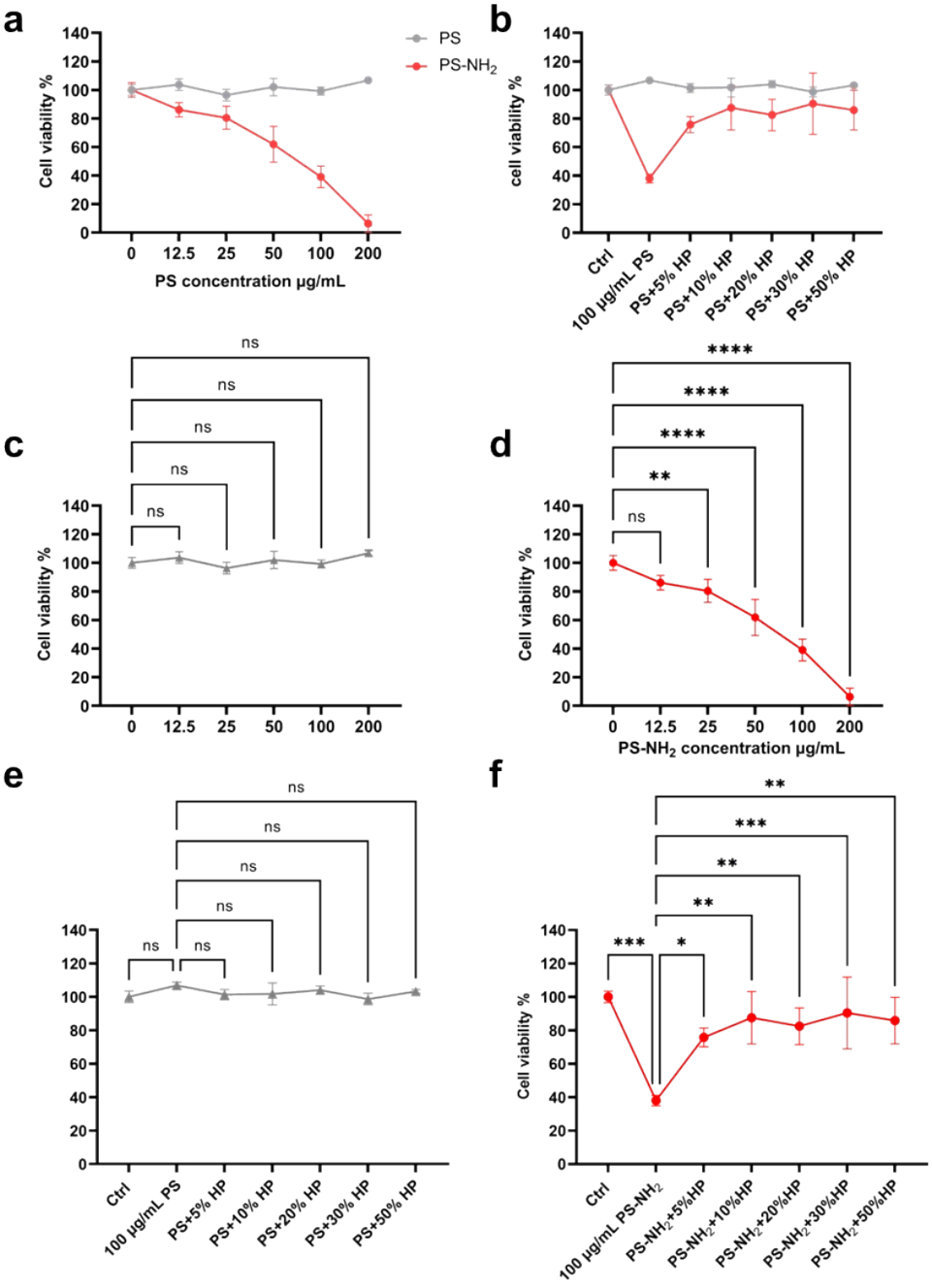

Figure S4. **The effect of PS NPs, PS-NH_2 NPs and their protein-coated forms on HEK-293 cell viability.** Cell viability of HEK-293 cells upon incubation with various concentrations of pristine PS or protein-coated PS for 72 h. Results are expressed as the percentage of living cells to untreated cells. Data are reported as mean ± SD, n⩾6. * p<0.05; ** p<0.01; ****p<0.0001, ordinary one-way ANOVA followed by Dunnett test.

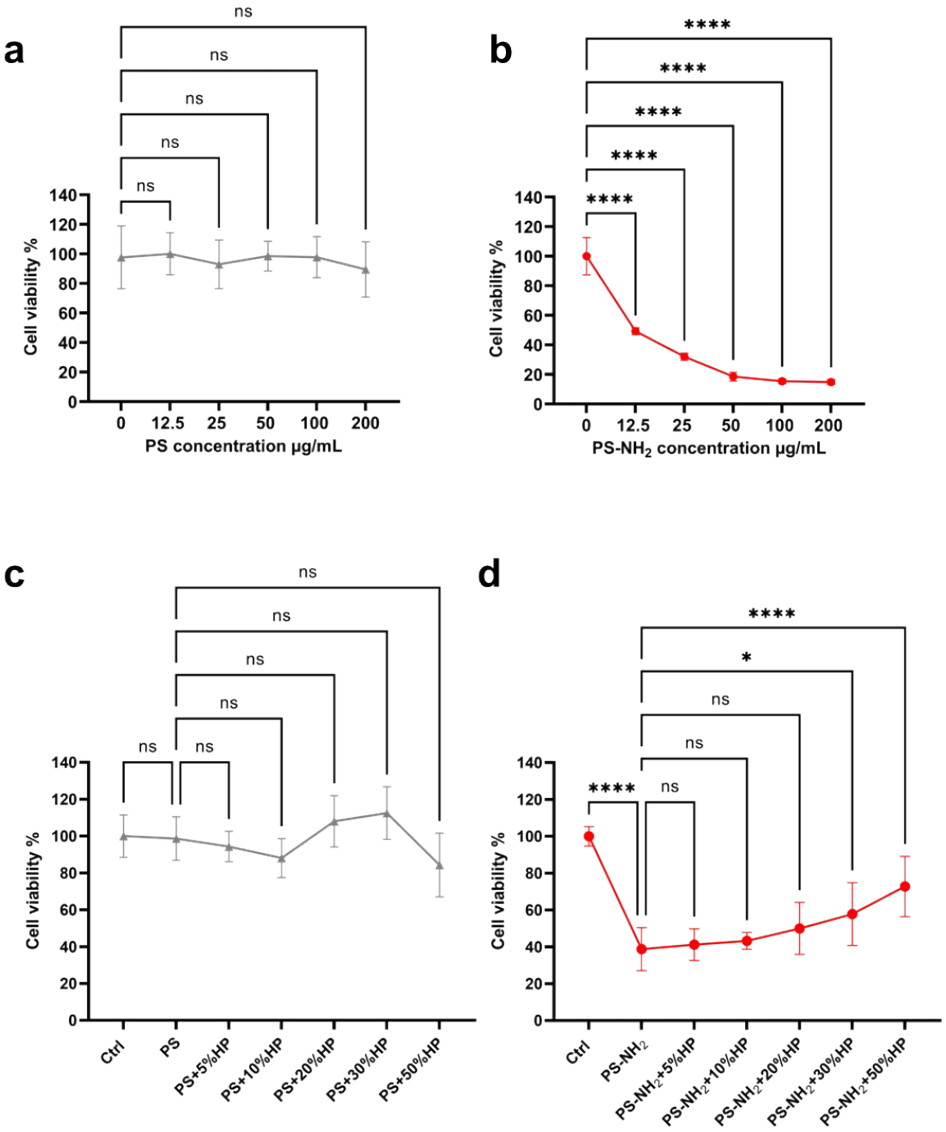

Figure S5. Statistical Analysis of cytotoxicity. Cell viability of SK-BR-3 cells upon incubation with various concentrations of pristine PS or protein-coated PS for 72 h. Results are expressed as the percentage of living cells to untreated cells. Data are reported as mean ± SD, n⩾6. * $p<0.05$; ** $p<0.01$; ****$p<0.0001$, ordinary one-way ANOVA followed by Dunnett test.

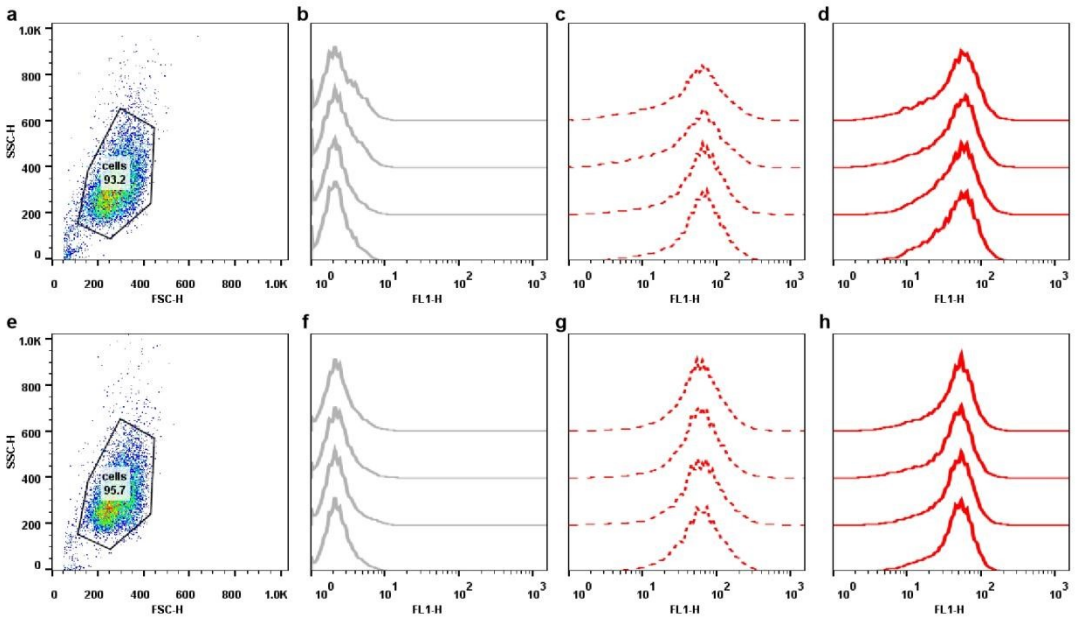

Fig S6. Gating strategy and histograms of the flow cytometry experiments. The results were obtained from two independent experiments (panel a-d from experiment 1 and e-h from experiment 2). SK-BR-3 cells were analyzed by forward scatter and sideward scatter to identify the cell population if interest and exclude cell debris, gating strategy was represented in panel a and e, and the gating was applied to all samples. PS-NH_2 NPs were labeled with an orange dye (Approximate Exi/Emi of 481/644 nm), and the events of the cell gate were analyzed for their fluorescence (excitation 488 nm, detected in FL1 channel, band-pass filter 530/30 nm). Within each experiment, we have 4 replicates, and the fluorescence distribution of control group (b, f), treated with pristine PS-NH_2 group (c,g), and treated with coronated PS-NH_2 group (d, h).

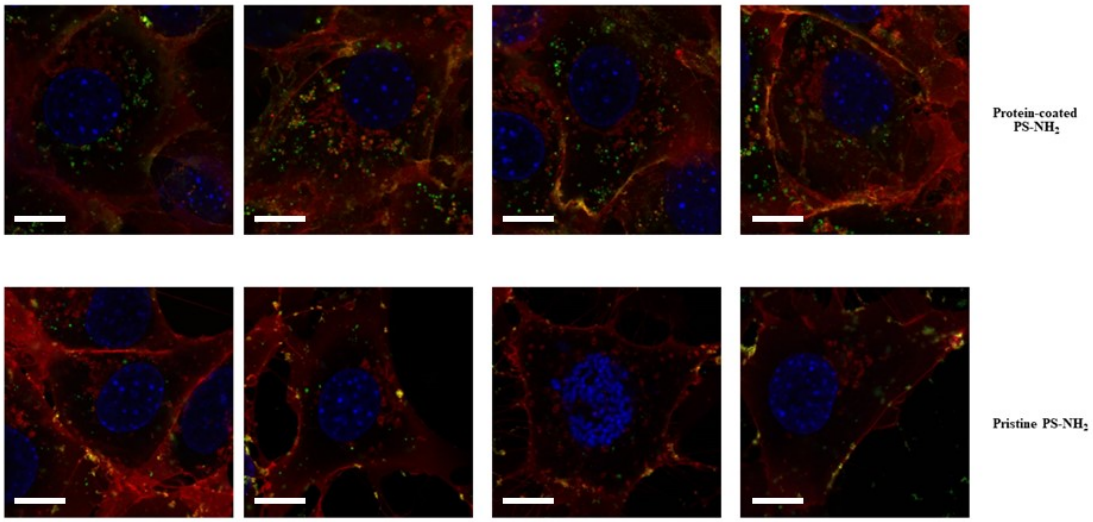

Fig. S7. Confocal microscopy images of 100 nm PS-NH_2 NPs internalized by NIH3T3 fibroblasts. NIH3T3 fibroblasts were treated under the same condition as SK-BR-3 cells, red represents CellMask™, blue represents nucleus stained with Hoechst 33,342, protein coated PS-NH_2 NPs and pristine PS-NH_2 NPs are indicated in green. Scale bars 10 μm. The results suggested the similar trend as observed in SK-BR-3 cells: pristine PS-NH_2 NPs tend to stick to the cell membrane, while protein pre-coating enhance their cellular uptake.

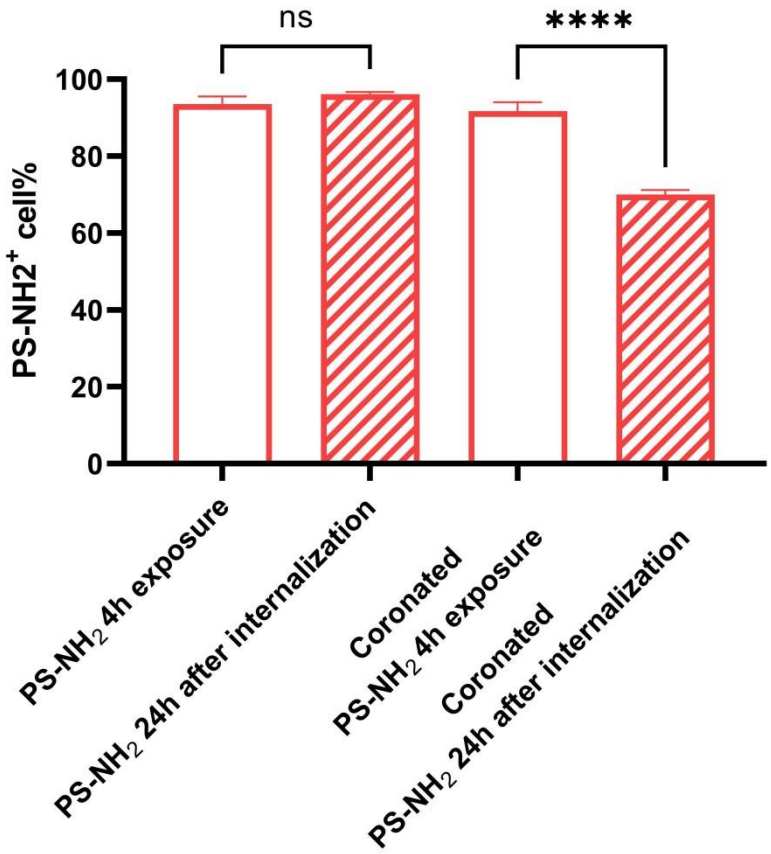

Fig S8. Cellular release of internalized PS-NH_2. SK-BR-3 cells were exposed to 12.5 μg/mL pristine or coronated PS-NH_2 NPs for 4h. After the exposure, the culture medium was removed, the cells were washed gently with PBS three times and replaced with PS-NH_2-free medium, 24 h after the replacement, cellular uptake was measured by PS-NH_2 positive cell percentage using flow cytometry. Data are reported as mean ± SD, n≥4. * $p<0.05$; ** $p<0.01$; ****$p<0.0001$, ordinary one-way ANOVA followed by Tukey test.

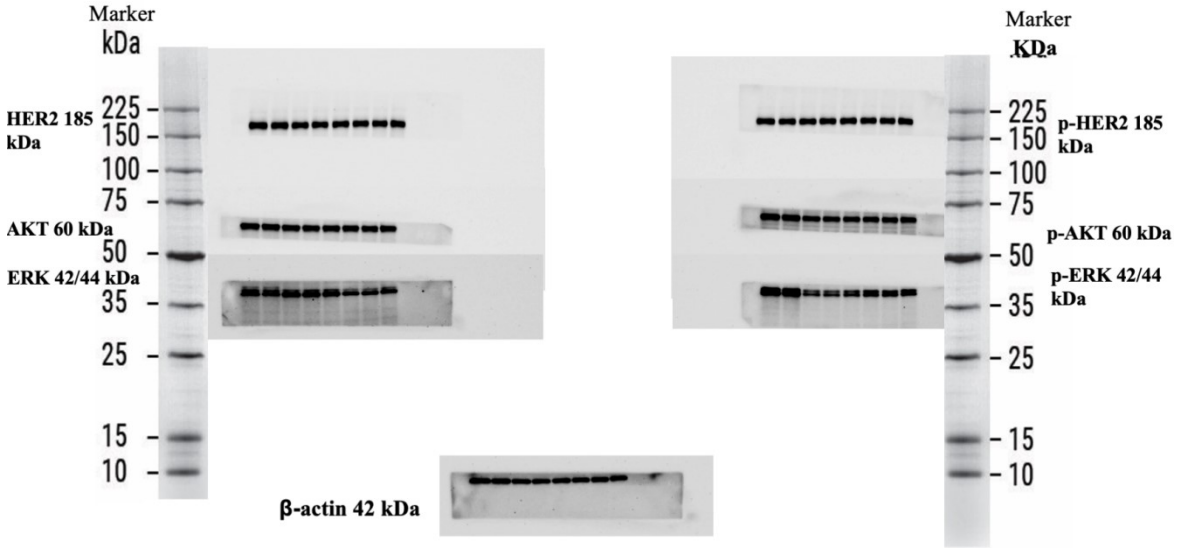

Fig. S9. Original western blots from which Figure 6 (Panel a) derived. Analysis of the expression levels of HER2, pHER2, AKT, pAKT, ERK, pERK and β-actin in SK-BR-3 cells treated or not with 12.5 μg/mL pristine or protein-coated PS-NH_2 for 24 h. Equal amounts of protein (20 μg) were loaded, and β-actin was used as loading control. Since β-actin and ERK have the same Molecular Weight, the membranes were stripped and re-blotted to detect β-actin. Samples were loaded as following order: control in duplicate, cell treated with 12.5 μg/mL PS-NH_2 in triplicate and coronated PS-NH_2 in triplicate.

References

1. Fang, J.; Xuan, Y.; Li, Q., Preparation of polystyrene spheres in different particle sizes and assembly of the PS colloidal crystals. *Science China Technological Sciences* **2010,** *53*, 3088-3093.
2. Araújo, R.; Ramalhete, L.; Ribeiro, E.; Calado, C., Plasma versus Serum Analysis by FTIR Spectroscopy to Capture the Human Physiological State. *BioTech* **2022,** *11* (4), 56.
3. Crocco, M. C.; Moyano, M. F. H.; Annesi, F.; Bruno, R.; Pirritano, D.; Del Giudice, F.; Petrone, A.; Condino, F.; Guzzi, R., ATR-FTIR spectroscopy of plasma supported by multivariate analysis discriminates multiple sclerosis disease. *Scientific Reports* **2023,** *13* (1), 2565.